

Impedance Matching for Multi-dimensional Open-system Photonic Crystals

Jun Ushida,^{1,2,*} Masatoshi Tokushima,² Masayuki Shirane,² Akiko Gomyo,² and Hirohito Yamada^{1,2}

¹*Optoelectric Industry and Technology Development Association (OITDA)*

²*Fundamental Research Laboratories, NEC Corporation, 34 Miyukigaoka, Tsukuba, 305-8501, JAPAN*

(Dated: June 11, 2021)

An electromagnetic (EM) Bloch wave propagating in a photonic crystal (PC) is characterized by the impedance (impedance and admittance) of the wave. The impedance is used to investigate transmission and reflection at a surface or an interface of the PC. In particular, the general properties of impedance are useful for clarifying the wave propagation characteristics. We give a general proof that the impedance of EM Bloch waves on a plane in infinite one- and two-dimensional (2D) PCs is real when the plane is a reflection plane of the PC and the Bloch wavevector is perpendicular to the plane. We also show that the pure-real feature of impedance on a reflection plane for an infinite three-dimensional PC is good approximation based on the numerical calculations. The analytical proof indicates that the method used for impedance matching is extremely simplified since only the real part of the impedance function is needed for analysis without numerical verification. As an application of the proof, we describe a method based on impedance matching for qualitatively evaluating the reflection at the surface of a semi-infinite 2D PC, at the interface between a semi-infinite slab waveguide (WG) and a semi-infinite 2D PC line-defect WG, and at the interface between a semi-infinite channel WG and a semi-infinite 2D PC slab line-defect WG.

PACS numbers: 42.70.Qs, 42.79.Gn

I. INTRODUCTION

Photonic crystals (PCs) are artificial materials whose dielectric functions periodically vary.^{1,2,3,4,5,6} The primary characteristics of PCs are photonic band gaps and peculiar dispersion relations, both of which enable the propagation of electromagnetic (EM) waves in PCs to be controlled. Recent interest in PCs has focused on “open-system PCs,”^{5,6,7,8,9,10,11} which are connected to other structures at their boundaries. Typically investigated are a finite PC contacting another medium and finite PC line-defect waveguides (WGs). In open-system PCs, the energy of propagating EM waves is transferred into or out of the PCs through the boundaries. This is in contrast to closed-system PCs, which are infinite in size and therefore contain all the energy at any time.

An open-system PC can be divided into a set of subsystems — the PC and the attached structures. Therefore, it should greatly facilitate designing open-system PCs if each subsystem is independently designed and then all the subsystems are assembled. Such a method has become well established for electrical circuit design. The behaviors of the electrical energy flows are predicted based on electrical impedance (impedance and admittance).¹² Two electrical circuits can be assembled without energy reflection at their interface if the electrical impedances of both circuits match. A complete electrical circuit system can thus be designed after designing each subsystem independently.

EM wave media including open-system PCs can be regarded as EM wave circuits, for which an analogous figure of merit, EM wave impedance, is similarly defined.¹³ It is a ratio of the electric field to the magnetic field of a propagating or decaying wave in a single medium. In practice, it has been possible to design one-dimensional

(1D) open-system PCs by using the EM wave impedance. Particularly notable is that the renormalized Fresnel coefficient for a semi-infinite 1D PC with an arbitrary unit cell has been defined using the EM wave impedance for Bloch waves.¹⁴ However, there is still difficulty in designing multi-dimensional open-system PCs. This is because the number of EM wave impedances that should be considered at a point on an arbitrarily shaped boundary increases with the number of structural dimensions. Specifically, the impedance of an EM wave with a given polarization is expressed as one parameter for a 1D PC, two parameters for a two-dimensional (2D) PC, and six parameters for a three-dimensional (3D) PC. Moreover, each parameter of an EM wave impedance is complex in general. Therefore, excessive computational cost would be needed to match every impedance parameter between two multi-dimensional subsystems.

One way to simplify the matching problem is to reduce the number of parameters by considering structural symmetry. Also, simplifying the parameters themselves is helpful, as has been suggested by Boscolo et al.¹⁵ They pointed out that a propagating wave in a PC line-defect WG has a pure-real impedance on periodic symmetry planes normal to the direction of propagation. Similar findings have been obtained through analytical calculation of the impedance of 1D PCs^{14,16} and through numerical calculation for 2D PCs.¹⁷ In this article, we take another approach to simplifying the matching problems — qualitative optimization of individual subsystems.

This paper is organized as follows. In Sec. II, we first prove that pure-real impedance is a common property of EM Bloch waves in 1D and 2D PCs, hence it can be used for any 1D or 2D open-system PC. We also prove that the pure-real property of the impedance is true for 3D periodic structures, but under a limiting con-

dition. Then, in Sec. III, we present three examples of designing multi-dimensional open-system PCs. This analysis can be made because the immittance defined by using eigenmodes on the boundary of two semi-infinite regions (a PC and its external structure) can be determined from the eigenmodes of an infinite PC and its external structure. In Sec. III A, we present a method for qualitatively evaluating the reflection at the surface of a semi-infinite 2D PC; the approximate availability of the perfect antireflection coating (ARC) method developed for a semi-infinite 1D PC¹⁴ to a semi-infinite 2D PC is emphasized. These semi-infinite 2D PCs can be used for analyzing various applications such as add/drop multiplexers, dispersion compensators, polarization filters, and image processors.^{4,18,19} In Sec. III B, we investigate a 2D line-defect WG that efficiently transmits EM energy to a channel WG. The semi-infinite 2D PC line-defect WG is a promising platform for ultra-compact photonic circuits.^{9,20} In Sec. III C, we investigate the interface between a semi-infinite channel WG and a semi-infinite 2D PC slab line-defect WG as a typical 3D problem.²¹ All the applications of the proof are presented using the concept of immittance matching. Section IV devotes for conclusion.

II. GENERAL PROOF FOR IMMITTANCE OF ELECTROMAGNETIC BLOCH WAVES

We begin our description of the proof with a general expression of EM Bloch waves. Assuming time harmonic EM waves, the general expression for an EM Bloch wave;⁶

$$\mathbf{E}(\mathbf{r}, t) = \mathbf{u}_{\mathbf{k}n}(\mathbf{r}) \exp(i\mathbf{k} \cdot \mathbf{r} - i\omega_{\mathbf{k}n}t), \quad (1)$$

$$\mathbf{H}(\mathbf{r}, t) = \mathbf{v}_{\mathbf{k}n}(\mathbf{r}) \exp(i\mathbf{k} \cdot \mathbf{r} - i\omega_{\mathbf{k}n}t), \quad (2)$$

where n and \mathbf{k} stand for the band index and Bloch wavevector, and functions $\mathbf{u}_{\mathbf{k}n}(\mathbf{r})$ and $\mathbf{v}_{\mathbf{k}n}(\mathbf{r})$ have lattice periodicity. The immittance of a Bloch wave is closely related to the energy flow conveyed by the wave; it is therefore useful to define a complex Poynting vector:

$$\mathbf{S}(\mathbf{r}) = \frac{1}{2} \mathbf{E}(\mathbf{r}, t) \times \mathbf{H}^*(\mathbf{r}, t) = \frac{1}{2} \mathbf{u}_{\mathbf{k}n}(\mathbf{r}) \times \mathbf{v}_{\mathbf{k}n}^*(\mathbf{r}), \quad (3)$$

where the real (imaginary) part of \mathbf{S} is the density of the time-averaged (reactive) power flow.²²

Here, we consider the time reversal state of Eqs. (1) and (2), which is written as

$$t' = -t \text{ and} \quad (4)$$

$$\mathbf{E}^{(\text{tr})}(\mathbf{r}, t') = \mathbf{E}(\mathbf{r}, -t), \quad (5)$$

$$\mathbf{H}^{(\text{tr})}(\mathbf{r}, t') = -\mathbf{H}(\mathbf{r}, -t), \quad (6)$$

due to the even (odd) parity of electric (magnetic) field under time reversal operation.²³ Eqs. (4)-(6) can be reduced to⁶

$$\omega_{-\mathbf{k}n} = \omega_{\mathbf{k}n} \quad (7)$$

$$\mathbf{u}_{-\mathbf{k}n}(\mathbf{r}) = \mathbf{u}_{\mathbf{k}n}^*(\mathbf{r}), \quad (8)$$

$$\mathbf{v}_{-\mathbf{k}n}(\mathbf{r}) = -\mathbf{v}_{\mathbf{k}n}^*(\mathbf{r}). \quad (9)$$

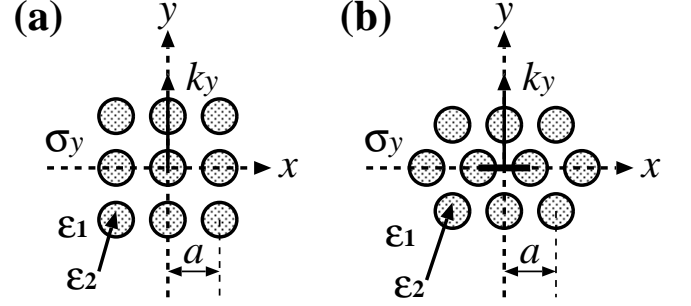


FIG. 1: Schematic illustration of typical infinite 2D PCs with reflection symmetry σ_y (at $y = 0$). (a) square lattice, (b) triangular lattice of circles with permittivity ϵ_2 and lattice constant a in medium with ϵ_1 .

Eqs. (7)-(9) express the time reversal degeneracy of the spin 1 particle (photon). Eqs. (7)-(9) will be used later.

Next, we consider a Poynting vector described using EM Bloch waves under a reflection operation in infinite 2D PCs. Figure 1 illustrates typical infinite 2D PCs with reflection plane σ_y . When the propagation direction of a Bloch wave is perpendicular to this plane, the electric Bloch wave $\mathbf{E}(\mathbf{r})$ is transformed by reflection operation into

$$\hat{O}_{\sigma_y} \mathbf{E}(\mathbf{r}) = IC_{2y} \begin{bmatrix} u_{nk_y,x} \\ u_{nk_y,y} \\ u_{nk_y,z} \end{bmatrix} (x, -y, z) e^{-ik_y y}, \quad (10)$$

$$= \begin{bmatrix} u_{nk_y,x}^* \\ -u_{nk_y,y}^* \\ u_{nk_y,z}^* \end{bmatrix} (x, -y, z) e^{ik_y y}, \quad (11)$$

where \hat{O}_{σ_y} , I , and C_{2y} stand for the σ_y reflection operator, the inversion operator, and the C_2 rotation about the y axis. Note that the obvious factor $\exp(-i\omega_{\mathbf{k}n}t)$ is omitted in Eqs. (10) and (11). Note also that this reflection operation (σ_y) is not the symmetry operation of the \mathbf{k} -group at $k_y \hat{\mathbf{e}}_y$, but of the point group in an infinite 2D PC. Similarly, magnetic Bloch wave $\mathbf{H}(\mathbf{r})$ is transformed into

$$\hat{O}_{\sigma_y} \mathbf{H}(\mathbf{r}) = \begin{bmatrix} v_{nk_y,x}^* \\ -v_{nk_y,y}^* \\ v_{nk_y,z}^* \end{bmatrix} (x, -y, z) e^{ik_y y}. \quad (12)$$

In the derivation of Eqs. (11) and (12), we use Eqs. (8) and (9). The non-zero components of EM waves in the Cartesian coordinate system are (H_x, H_y, E_z) for TM and (E_x, E_y, H_z) for TE polarization.²⁴

Accordingly, the Poynting vector described using the EM Bloch wave under reflection operation can be written as

$$S_y^{(\sigma_y)}(\mathbf{r}) = \begin{cases} u_{nk_y,z}^* v_{nk_y,x}/2 & (\text{for TM}) \\ -u_{nk_y,x}^* v_{nk_y,z}/2 & (\text{for TE}) \end{cases}. \quad (13)$$

On reflection plane $y = 0$, $S_y^{(\sigma_y)}(x, 0, z)$ equals $S_y(x, 0, z)$. Therefore, using Eqs. (3) and (13), we obtain

$$S_y(x, 0, z) = S_y^{(\sigma_y)}(x, 0, z) \quad (14)$$

$$\Leftrightarrow \begin{cases} \frac{u_{nk_y,z}}{v_{nk_y,x}} = \left(\frac{u_{nk_y,z}}{v_{nk_y,x}} \right)^* & (\text{for TM}) \\ -\frac{u_{nk_y,x}}{v_{nk_y,z}} = -\left(\frac{u_{nk_y,x}}{v_{nk_y,z}} \right)^* & (\text{for TE}) \end{cases} \quad (15)$$

$$\Leftrightarrow \begin{cases} \text{Im}(Z_{zx}) = 0 & (\text{for TM}) \\ \text{Im}(Z_{xz}) = 0 & (\text{for TE}) \end{cases}, \quad (16)$$

where $Z_{zx} \equiv u_{nk_y,z}/v_{nk_y,x}$, and $Z_{xz} \equiv -u_{nk_y,x}/v_{nk_y,z}$ at $(x, 0, z)$.

Q. E. D.

Eq. (16) means that the immittance is real in infinite 1D and 2D PCs on a plane when the plane is a reflection plane and the Bloch wavevector is perpendicular to the plane. It also means that the reactive power flow is zero for the Bloch wave on the plane under consideration.

For the case of an infinite 3D PC, Eq. (14) can be written as

$$u_{nk_y,z}v_{nk_y,x} - u_{nk_y,x}v_{nk_y,z} = (u_{nk_y,z}v_{nk_y,x} - u_{nk_y,x}v_{nk_y,z})^*. \quad (17)$$

Therefore, an additional reflection plane is required for removing the imaginary part of the impedance. When there is reflection plane σ_z at $z = 0$, some components of the EM waves vanish on the plane. They are called TM- or TE-like based on the analogy to infinite 2D PCs.²⁵ In this case, the impedance is real on the intersection line of the $y = 0$ and $z = 0$ planes.

III. APPLICATIONS OF PURE-REAL PROPERTY OF IMMITTANCE

As a typical application of the above proof, we present a method reducing a reflection loss at the surface of a semi-infinite 2D PC, a semi-infinite 2D PC line-defect WG, and a semi-infinite 2D PC slab line-defect WG based on the concept of the immittance matching. The method for the immittance matching is extremely simplified since only the real part of immittance function for an infinite PC is needed for the analysis. The reflection coefficient of a semi-infinite PC should be determined via Bloch wave expansion in the semi-infinite PC and the expansion should be described by all the eigen modes of an infinite PC (i.e., including decaying waves).²⁶ However, here we investigate only the impedance of propagation modes. This is another merit of our method, that is, it is not necessary to know all the eigenmodes in our method for immittance matching problem. The information on the impedance of propagation modes can be used for qualitatively investigating the reflection in various types of open system PCs.

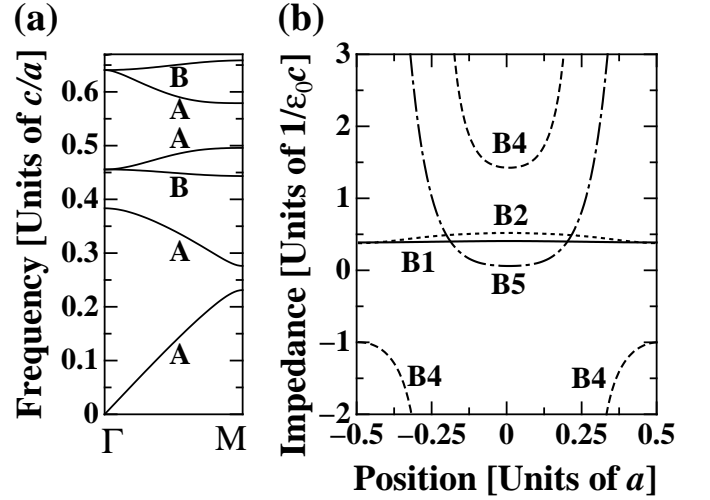


FIG. 2: (a) Dispersion relation of TM wave in ΓM direction for infinite 2D PC with triangular lattice of air holes ($\epsilon_2 = 1$). Permittivity ϵ_1 is 11.9025 and hole radius is $0.4335a$, where a is lattice constant. Index “A” (“B”) indicates the coupled (uncoupled) mode.^{28,29,30} (b) Normalized impedance of Bloch waves with $k_y = 2\Gamma M/3$ at $y = 0$. We use index B1-B5 (band number) to label the modes in order of increasing frequency. Only Bloch waves that coupled with an external plane wave are shown.

A. Semi-infinite 2D PC

The geometry of the first example is shown in Fig. 1 (b). The parameters of the PC is summarized in the caption of Fig. 2.

Figure 2 (a) illustrates the dispersion relation of the TM polarization wave for the infinite 2D PC in the ΓM direction.²⁷ Suppose that one considers the reflection at the surface of a semi-infinite PC made from the infinite PC cleaved at the plane $y = 0$ shown in Fig. 2 (b). The incident wave is a normal incident plane wave propagating in vacuum. Then, one should calculate the immittance of the Bloch wave at $y = 0$ by using the eigen mode of the infinite PC. The immittance of the Bloch wave is generally complex and has lattice periodicity of the infinite 2D PC. The impedance at $y = 0$ calculated using propagating Bloch waves with $k_y = 2\Gamma M/3$ is shown in Fig. 2 (b). The illustrated region is indicated by the thick solid line in Fig. 1 (b). The impedance is normalized by the impedance in vacuum. Note that only the impedance of Bloch waves able to couple with an incident plane wave (“coupled modes”) indicated by “A” in Fig. 2(a) is plotted. Since the spatial modulation of bands B1 and B2 is flatter than that of bands B4 and B5 and the impedance is near the value in vacuum (i.e. impedance normalized by vacuum value is near one), the reflection loss of bands B1 and B2 at the frequency is lower than that of bands B4 and B5 for the normal incidence of a plane wave. In addition, the flatness of the impedance enables us to reduce the reflection loss by using an antireflection coating (ARC) method developed for semi-infinite 1D PCs.¹⁴ In

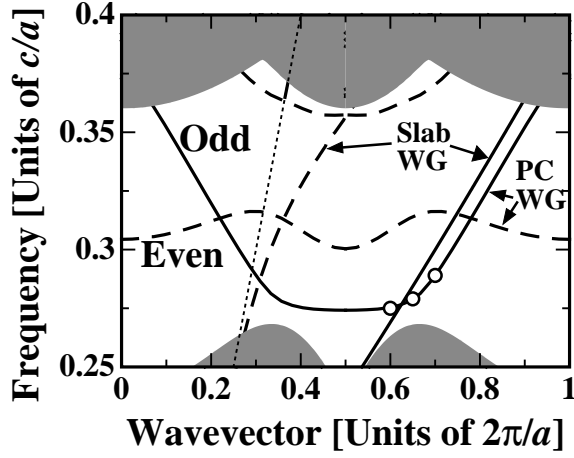


FIG. 3: Dispersion relation of infinite slab waveguide (WG) and infinite PC WG. PC has triangular lattice of air holes, with radius $r = a/3$ in medium with $\epsilon_2 = 7.6176$. Even (odd) mode under reflection operation σ_x bisecting WGs is shown as solid (broken) line. Circles show points equivalent to $K = -0.30, -0.35$, and -0.40 , which are used to calculate impedances shown in Figs. 4(a) and (b).

this case, since the plane $y = 0$ is a reflection plane, thickness d and refractive index n_2 of the ARC can be estimated using

$$D \equiv \frac{d}{\lambda_0/4n_2} = 1, 3, 5, \dots \quad \text{and} \quad (18)$$

$$n_2 \simeq \sqrt{n_1 \text{Re}(Y_{zx})/\epsilon_0 c} \quad \text{at } x, y = 0, \quad (19)$$

where D is the normalized thickness of the ARC, λ_0 is a wavelength in vacuum, n_1 is the refractive index of a semi-infinite medium, and $Y_{zx} \equiv 1/Z_{zx}$ for TM polarization. Accordingly, the reflection loss is easily removed by using Eqs. (18) and (19). If a spatially flat impedance appears in the TE polarization case, Eq. (19) can be used by replacing Y_{zx} with $Y_{xz} \equiv 1/Z_{xz}$ to reduce the reflection loss of the TE polarization waves.

B. Semi-infinite 2D Line-defect PC Waveguide

The second example is related to the interconnection between a semi-infinite slab waveguide (WG) and a semi-infinite 2D PC line-defect WG, or “PC WG.” The connection between different WGs is important to realize the ultra-minute photonic circuits. Although some numerical investigation were made for similar structures,^{20,21,31,32,33,34,35} we investigate it based on the concept of immittance matching. The semi-infinite PC WG is made by removing a row of air holes in the ΓK direction from a semi-infinite 2D triangular lattice of air holes with radius $r = a/3$ and $\epsilon_2 = 1$ in a medium with $\epsilon_1 = 7.6176$. The slab WG has width $\sqrt{3}a - 2r$ and permittivity $\epsilon = 7.6176$ (the same as the ϵ_1 of the PC). The dispersion relation of the propagation modes of the

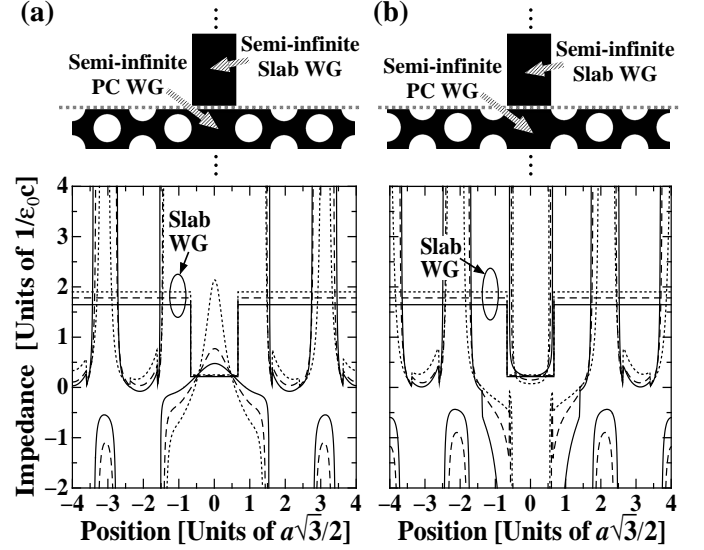


FIG. 4: Dependence of spatial distribution of impedance on wavevector and on surface of semi-infinite PC WG. Difference between Figs. 4 (a) and (b) is the position of the surface of semi-infinite PC line-defect WG connected with semi-infinite slab WG, shown as dotted line in diagram³⁷ above each graph. Wavevector dependence is shown as solid (normalized wavevector $K = -0.30$), dashed ($K = -0.35$), and dotted ($K = -0.40$) lines. The rectangular impedance distribution is impedances for slab WG with width $\sqrt{3}a - 2r$.

infinite slab WG and infinite PC WG are shown in Fig. 3.²⁷ The polarization is TE; that is, the magnetic wave is parallel to the slab and to the axis of air holes in the infinite 2D PC.²⁴ Since the both of the slab WG and the PC WG have reflection plane bisecting these WGs, the propagation mode has even (broken line) or odd (solid line) parity under reflection operation, as shown in Fig. 3. The shaded region indicates the projection band structure. When $K = 0.6 \sim 0.9$, the dispersion relation of the infinite slab WG is similar to that of the infinite PC WG. Such situation was called **k**-matching (wavevector matching) by Mekis et al.^{34,35} as a mechanism to reduce the reflection from the joint of a distributed Bragg reflector WG and a 2D PC WG with square lattice of rods. On the other hand, the exactly derived renormalized Fresnel coefficients of a semi-infinite 1D PC did not include Bloch wavevector explicitly.¹⁴ The analytical investigation of a relation between immittance matching and **k**-matching will be published elsewhere.³⁶

Here, we investigate the direct connection between a semi-infinite slab WG and a semi-infinite PC WG based on the immittance matching. Figure 4 illustrates the dependence of the spatial distribution of the impedance on the wavevector and on the surface of the semi-infinite PC WG. The difference between Figs. 4 (a) and (b) is the position of the surface [shown as a dotted line in the diagram above each graph in Figs. 4(a) and (b)] of the semi-infinite PC WG connected with the semi-infinite slab WG. For the semi-infinite slab WG, the

impedance is homogeneous inside and outside the slab region, which shows a rectangular spatial distribution. In addition, the impedance at a surface is independent of the cleaved position of the infinite slab WG. For the semi-infinite PC WG, the impedance depends strongly on the position of the surface of the semi-infinite PC WG due to the spatial periodicity of the impedance in the infinite PC WG. Moreover, the impedance on a surface has a complex spatial distribution on the surface. Divergence appears where the magnetic wave vanishes. Divergence in a differential impedance appears at normalized position $X \equiv 2x/\sqrt{3}a = \pm 2 \pm 2/3\sqrt{3}, \pm 4 \pm 2/3\sqrt{3} \dots$ for Fig. 4 (a), and at $\pm 1 \pm 2/3\sqrt{3}, \pm 3 \pm 2/3\sqrt{3} \dots$ for Fig. 4 (b). The divergence is due to the discontinuity of the electric wave perpendicular to the air holes at the surface of the semi-infinite PC WG. From the Poynting vector calculation, we can confirm that the EM energy of these propagation modes concentrates around the normalized position $X = 0$.¹⁵ Therefore, region $X = -1 + 2/3\sqrt{3} \sim 1 - 2/3\sqrt{3}$ (\sim the width of the slab WG) is quite important for analyzing the immittance matching between the semi-infinite slab WG and semi-infinite PC WG modes. In this region, the impedance matching between the semi-infinite slab WG and the semi-infinite PC WG modes of Fig. 4 (b) is better than that of Fig. 4 (a). Hence, the geometry of Fig. 4 (b) is better for reducing reflection loss. In addition, when the wavevector approaches the 1st Brillouin zone boundary, the difference in the impedance between the slab WG and the PC WG modes becomes noticeable. Therefore, in a direct interconnection between the semi-infinite slab WG and the semi-infinite PC WG, the reflection loss of modes with $K = -0.4$ is higher than that with $K = -0.3$.

C. Application to 3D structures –Semi-infinite 2D PC Slab Line-defect WG–

In this section, we investigate the connection between a semi-infinite 2D PC slab line-defect WG and a semi-infinite channel WG based on the concept of immittance matching. Schematic illustrations of two kinds of connections are shown in Figs. 6 (a) and (b). The structures are sandwiched by two semi-infinite vacuum regions in the vertical direction (x -axis direction), hence they are 3D in nature. The 2D PC slab consists of a triangular lattice of air holes. The line defect WG is introduced into the slab by filling the air holes in a row. The detailed parameters of these structures are given in the caption of Fig. 5. The width and thickness of the channel WG are $\sqrt{3}a - 2r$ and $0.6a$, where r is the radius of the air holes and a is the lattice constant.

Figure 5 illustrates the energy dispersion relation of the TE-like modes of an infinitely long 2D PC line-defect WG. Fundamental EM mode propagating in the channel WG can be coupled only with the “odd” modes of 2D PC slab WG in the ideal case [Mode symmetry is defined by

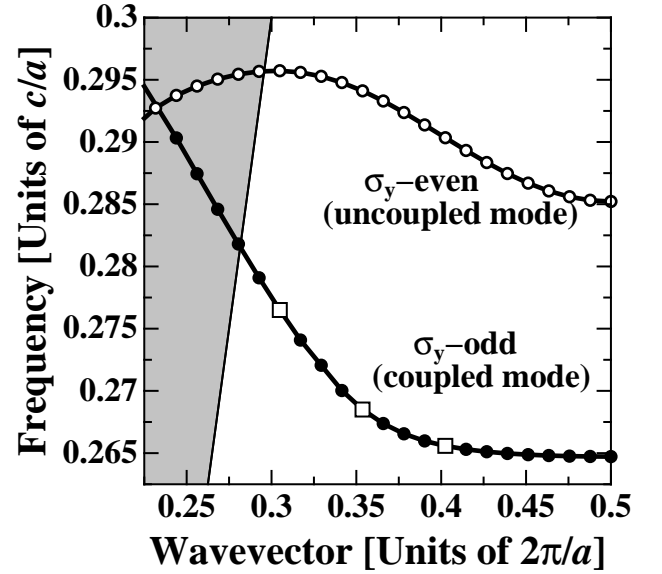


FIG. 5: Dispersion relation of TE-like modes of 2D PC slab line-defect WG. The slab consists of the triangular lattice of air holes (radius $r = 0.29a$, thickness $h = 0.6a$, refractive index $n = 3.4$, where a is the lattice constant). The line defect is introduced by filling up a row of air holes. These parameters are the same as in Ref. 38. The 3D calculations are needed for this structure.²⁷ The symmetry of the non-leaky guided modes is indicated as σ_y -even or -odd, where σ_y indicates the symmetry plane at $y = 0$ in Fig. 6 (a) and (b). Squares stand for points executing impedance calculations shown in Figs. 6 (a) and (b).

the symmetry operation associated with the symmetry plane (σ_y at $y=0$) bisecting the 2D PC slab WG and the channel WG]. Therefore, we consider the odd mode only hereafter.

Even if the structures of the 2D PC slab WG and the channel WG were fixed, there would still be ambiguity in determining the structure of the connection — the position of the cutting surface in a unit cell of a 2D PC slab WG. This situation is the same as the 2D problem in Sec. III B. If we select a reflection plane as the cutting surface, there are two possible choices, as illustrated in Figs. 6 (a) and (b) (at $z = +0$). To illustrate their difference more precisely, we show the top views ($x = 0$ plane) and the side views ($z = 0$ plane) of the refractive index distribution in the unit cell used for the supercell calculations²⁷ in Figs. 6 (c)-(f); black indicates the regions with refractive index $n = 3.4$, and white indicates the region with vacuum. The size of the supercell used in our calculation can be obtained from these figures.

When a 2D PC slab WG is terminated and connected with a semi-infinite channel WG at $z = 0$, the immittance distribution should be calculated at $z = +0$. The analytical results presented in Sec. II show that the pure-real feature of immittance on a symmetry plane for a 3D structure is preserved along a particular line only. However, our numerical results indicate that the imaginary

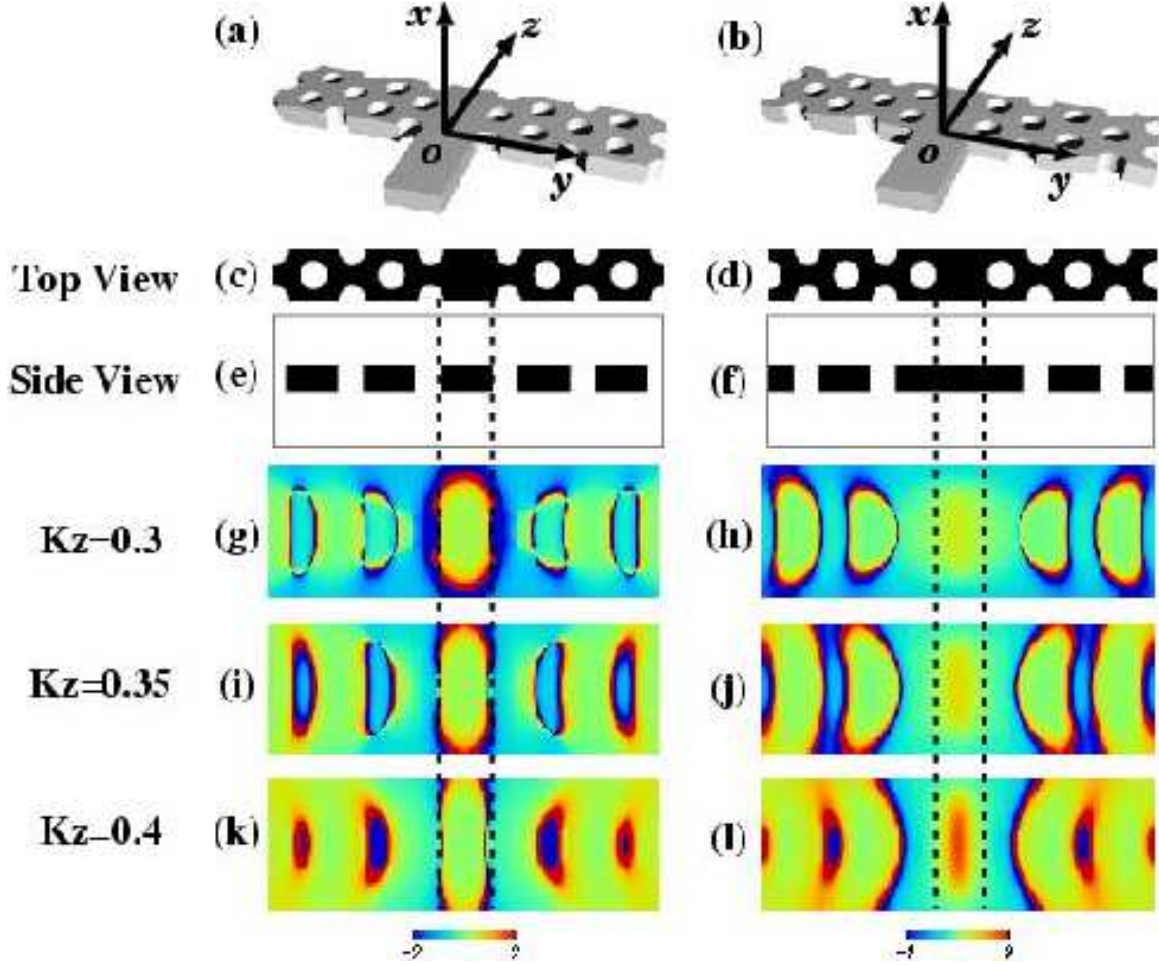


FIG. 6: Dependence of spatial distribution of impedance on wavevector and on surface of semi-infinite 2D PC slab line-defect WG. Difference between Figs. 6 (a) and (b) is the position of the surface of semi-infinite PC slab line-defect WG connected with semi-infinite channel WG ($z = +0$). (c)-(f): top and side views of refractive index distribution. (g)-(l): Dependence of impedance $\text{Re}[Z_{yx}]$ (in units of $1/\epsilon_0 c$) on cutting surface and Bloch wave vector. The dotted lines indicate the width of the channel WG.

part of immittance on a symmetry plane is much smaller than the real part. In this situation, the imaginary part of the immittance on a symmetry plane is negligible in qualitative immittance matching analysis. Moreover, additional components of the immittance appear in the 3D problem. This is because all components of an EM field cannot be treated separately. The two possible combination of EM fields in the impedance calculation for Bloch waves propagating in the z direction are

$$Z_{yx}(x, y, +0) = -\frac{E_{k_z, y}(x, y, +0)}{H_{k_z, x}(x, y, +0)}, \quad (20)$$

$$Z_{xy}(x, y, +0) = \frac{E_{k_z, x}(x, y, +0)}{H_{k_z, y}(x, y, +0)}. \quad (21)$$

Since we use TE-like mode only in this analysis, Z_{xy} is much smaller than Z_{yx} , and this was confirmed by our numerical calculations. Therefore, in Figs. 6 (g)-(l) we illustrate the real part of impedance distribution Z_{yx} at

$z = +0$. The regions of these plots are the same as those in Figs. 6 (e) and (f). The value of $\text{Re}[Z_{yx}]$ is colored linearly. Note that the region $|\text{Re}[Z_{yx}]| \geq 2$ is colored red or blue. Note also that the energy dispersion relation of the odd mode shown in Fig. 5 has negative group velocity, so the impedance is calculated by using time reversal states of EM fields.

The results presented in Sec. IIIB clearly show that the structure in Fig. 6 (a) is more suitable for low-loss connections than that in Fig. 6 (b). This is supported by 3D calculations of the impedance distribution around the WG region $[-(\sqrt{3}a - r) \leq y \leq \sqrt{3}a - r]$ (between dotted lines in Fig. 6). The impedance distribution shown in Fig. 6 (g) is flatter than that in (h) at this region; meaning that the structure in (a) has lower reflection than that in (b).

Next, we investigate their dependence on the Bloch wavevector, which is also shown in Figs. 6 (g)-(l). When the length of the Bloch wavevector increases, the regions

colored red and blue expand. This means that the regions with $|\text{Re}[Z_{yz}]| \geq 2$ expand, so the reflectance of EM waves increases.

IV. CONCLUSION

In conclusion, we presented a qualitative method for evaluating the reflection of multi-dimensional semi-infinite PCs that is based on the concept of immittance matching. Using the analytical investigation of Poynting vectors defined using Bloch waves, we presented a general proof that the imaginary part of the complex immittance on periodic planes is zero in infinite 1D and 2D PCs when the plane is a reflection plane and the Bloch wavevector is perpendicular to the plane. The infinite 3D PC case was also analyzed. To show the usefulness of this proof, we presented a qualitative method for evaluating reflection loss (a) at the surface of semi-infinite 2D PCs, (b) at the interface between a semi-infinite slab WG and a semi-infinite PC line-defect WG, and (c) at the interface between a channel WG and a semi-infinite 2D PC slab line-defect WG. The first example showed approximate applicability of the ARC method developed for semi-infinite 1D PCs to semi-infinite multi-dimensional PCs. The second example showed that the use of a connection with the geometry shown in Fig. 4 (b) reduces the reflection. The third example showed that the pure-real feature of the immittance is a good approximation on a symmetry plane of 2D PC slab WG.

Note that reflection of PCs is sometimes discussed

in relation with the group velocity or the density of states in the infinite PC. While this can provide good physical intuition, we need to remember that the reflectance strongly depends on the structure of the surface of a PC. The immittance of EM Bloch wave is essential for the discussion of the reflection phenomena for any “open-system” PCs. The general concept of immittance matching was used for this theoretical prediction and is well suited for reflection and transmission analysis for a wide variety of “open-system” PCs.

Acknowledgments

We thank Dr. Eiji Miyai and Professor Susumu Noda for showing us their work (See, Ref. 37) before publication. They also thank Mr. Arnold Fisher for his critical reading of manuscript. One of authors (J.U.) thanks Dr. Steven G. Johnson for useful comments to the relation among adiabatic interconnections, \mathbf{k} -matching, and impedance matching at private communication in Tsukuba, Japan on 19 Dec. 2002. We thank Kazuo Nakamura and Jun'ichi Sone for their support. This work was done as part of the “Photonic Network Project” under contract from the New Energy and Industrial Technology Development Organization (NEDO) and Focused Research and Development Project for the Realization of the World's Most Advanced IT Nation, IT Program, MEXT.

-
- * Electronic address: ushida@cj.jp.nec.com
- ¹ E. Yablonovitch, Phys. Rev. Lett. **58**, 2059 (1987).
 - ² S. John, Phys. Rev. Lett. **58**, 2486 (1987).
 - ³ K. Ohtaka, Phys. Rev. B **19**, 5057 (1979).
 - ⁴ H. Kosaka, T. Kawashima, A. Tomita, M. Notomi, T. Tamamura, T. Sato, and S. Kawakami, Appl. Phys. Lett. **74**, 1370 (1999); Phys. Rev. B **58**, 10096 (1998).
 - ⁵ J. D. Joannopoulos, R. D. Meade, and J. N. Winn, *Photonic Crystals: Molding the Flow of Light* (Princeton University Press, Princeton, NJ, 1995).
 - ⁶ K. Sakoda, *Optical Properties of Photonic Crystals* (Springer, Berlin, 2001).
 - ⁷ S. Noda, A. Chutinan, and M. Imada, Nature **407**, 608 (2000).
 - ⁸ A. Mekis, J. C. Chen, I. Kurland, S. Fan, P. R. Villeneuve, and J. D. Joannopoulos, Phys. Rev. Lett. **77**, 3787 (1996).
 - ⁹ S. G. Johnson and J. D. Joannopoulos, *Photonic Crystals: The Road from Theory to Practice* (Kluwer Academic Publishers, Boston, 2002).
 - ¹⁰ N. Stefanou and A. Modinos, Phys. Rev. B **57**, 12127 (1998).
 - ¹¹ V. Yannopapas, A. Modinos, and N. Stefanou, Phys. Rev. B **65**, 235201 (2002).
 - ¹² O. Heaviside was the first to use the word “impedance” in 1886 and “admittance” in 1887. The word “immittance” was first used by D. Woods in 1957 according to *The Oxford English Dictionary* 2nd Ed. (Clarendon Press, Oxford, 1989).
 - ¹³ S. A. Shelkunoff, Bell Syst. Tech. J. **17**, 17 (1938).
 - ¹⁴ J. Ushida, M. Tokushima, M. Shirane, and H. Yamada, Appl. Phys. Lett. **82**, 7 (2003).
 - ¹⁵ S. Boscolo, C. Conti, M. Midrio, and C. G. Someda, J. Lightwave Tech. **20**, 304 (2002).
 - ¹⁶ S. Kawakami (private communication at “Photonic Crystals and Quantum Dots” symposium held in Tokyo, Japan on 17-18 Mar. 2003).
 - ¹⁷ S. Noda (private communication).
 - ¹⁸ Y. Ohtera, T. Sato, T. Kawashima, T. Tamamura, and S. Kawakami, Electron. Lett. **35**, 1271 (1999).
 - ¹⁹ M. Notomi, Phys. Rev. B **62**, 10696 (2000).
 - ²⁰ H. Yamada, M. Tokushima, and M. Shirane, Proc. SPIE, **4870**, 357 (2002).
 - ²¹ E. Miyai, M. Okano, M. Mochizuki, and S. Noda, Appl. Phys. Lett. **81**, 3729 (2002).
 - ²² R. M. Fano, L. J. Chu, and R. B. Adler, *Electromagnetic Fields, Energy and Forces* (Wiley, New York, 1960) p. 322.
 - ²³ J. D. Jackson, *Classical Electrodynamics*, 3rd ed. (Wiley, New York, 1999) p. 271.
 - ²⁴ Based on the definition of TM and TE modes in J. D. Joannopoulos, R. D. Meade, and J. N. Winn, *Photonic*

- Crystals: Molding the Flow of Light* (Princeton University Press, Princeton, NJ, 1995) p. 104.
- ²⁵ S. G. Johnson, S. Fan, P. R. Villeneuve, J. D. Joannopoulos, and L. A. Kolodziejski, Phys. Rev. B **60**, 5751 (1999).
 - ²⁶ T. Minami, H. Ajiki, and K. Cho, Physica E (Amsterdam) **13**, 432 (2002).
 - ²⁷ Calculation was done using the MIT Photonic-Band program developed by Steven G. Johnson. Refer to <http://ab-initio.mit.edu/mpb>; Steven G. Johnson and J. D. Joannopoulos, Opt. Express **8**, 173 (2001).
 - ²⁸ W. M. Robertson, G. Arjavalingam, R. D. Meade, K. D. Brommer, A. M. Rappe, and J. D. Joannopoulos, Phys. Rev. Lett. **68**, 2023 (1992).
 - ²⁹ W. M. Robertson, G. Arjavalingam, R. D. Meade, K. D. Brommer, A. M. Rappe, J. D. Joannopoulos, J. Opt. Soc. Am. B, **10**, 322 (1993).
 - ³⁰ K. Sakoda, Phys. Rev. B **52**, 7982 (1995).
 - ³¹ Y. Xu, R. K. Lee, and A. Yariv, Opt. Lett. **25**, 755 (2000).
 - ³² A. Adibi, Y. Xu, R. K. Lee, A. Yariv, and A. Scherer, J. Lightwave Technol. **18**, 1554 (2000).
 - ³³ A. Adibi, Y. Xu, R. K. Lee, A. Yariv, and A. Scherer, Phys. Rev. B **64**, 033308 (2001).
 - ³⁴ A. Mekis and J. D. Joannopoulos, J. Lightwave Technol. **19**, 861 (2001).
 - ³⁵ A. Mekis, S. Fan, and J. D. Joannopoulos, IEEE Microwave Guid. Wave Lett. **9**, 502 (1999).
 - ³⁶ M. Tokushima, J. Ushida, and H. Yamada (to be published).
 - ³⁷ Our surface structure is similar to, but different from, the structure proposed by E. Miyai, M. Okano, M. Mochizuki, and S. Noda (private communication at poster session of Int. Conf. on Solid State Devices and Materials held in Nagoya, Japan on 17 Sep. 2002, unpublished); E. Miyai and S. Noda (to be published).
 - ³⁸ A. Chutinan and S. Noda, Phys. Rev. B **62**, 4488 (2000).